Positronium thermalization in SiO_2 powder

A. P. Mills, Jr., E. D. Shaw, R. J. Chichester, and D. M. Zuckerman
AT&T Bell Laboratories, Murray Hill, New Jersey 07974
(Received 6 February 1989)

Slow positron pulses are implanted at variable energies into a SiO_2 powder target to form positronium (Ps). By time-of-flight methods we estimate the energy spectrum of the Ps that diffuses out of the target into the vacuum. As expected, higher implantation energies and lower target temperatures result in a colder Ps energy spectrum. However, even with 19-keV positron implantation energies, the Ps escaping from a target at 4.2 K is only about 2% thermalized. No evidence was found for a low-energy cutoff due to Ps localization between the powder grains.

I. INTRODUCTION

For a number of reasons it would be advantageous to have a source of positronium (Ps) in vacuum with kinetic energies much lower than the near room temperature Ps that can be produced by thermal desorption from metal surfaces.[1] Precision Ps spectroscopy,[2] gravitational free fall experiments, and various quantum projects such as the study of Ps Bose condensation, Ps localization, and Ps sticking probabilities, all require a source of cold Ps. One possible source might be the Ps that is emitted from the surface of a cold powder target, since collisions of Ps with the powder grains provide a mechanism for thermalization. An interesting advantage of studying powders is that at sufficiently low temperatures the Ps should become localized due to strong scattering. The localization might be visible as a low-energy cutoff in the velocity spectrum of the Ps escaping from the powder.

It is now more than two decades since Paulin and Ambrosino discovered that nearly free positronium (Ps) is formed when energetic positrons are implanted into a powdered insulator target.[3] The effect was explained by Brandt and Paulin[4] as being due to Ps forming within a powder grain, diffusing to the grain surface, and escaping into the voids between the grains. A further development was the observation by Curry and Schawlow[5] of Ps emitted into the vacuum away from a thin MgO powder surface irradiated by energetic positrons, and the estimate by them of the Ps kinetic energy, 0.28 eV. A few years later, a maximum axial component of the kinetic energy of about 0.8 eV was found by Gidley *et al.*[6] in a time-of-flight measurement of the velocity spectrum of the Ps emitted by a MgO powder surface irradiated by 400-eV slow positrons. Chang *et al.*[7] found a similar value of the kinetic energy for the Ps emitted by silica aerogel and pointed out that the kinetic energy may be interpreted as the negative of the Ps work function, ϕ_{Ps}. Most recently, Sferlazzo, Berko, and Canter[8] measured the Ps work function for solid quartz crystals and found $\phi_{Ps}=-3.27(4)$ eV.

In none of the above experiments to measure the Ps kinetic energy did the Ps emerge after diffusing through a thick powder layer, either because the layer itself was thin,[5] or because low implantation energies were used.[6] It is likely that the Ps emerging from deep within a thick layer would have kinetic energies representative of the temperature of the powder, rather than of the Ps negative work function. The purpose of the present experiment is to investigate the conditions necessary for the thermalization of emerging Ps, and the limitations on how cold the Ps may be. Accordingly we have implanted positrons into a thick layer of SiO_2 powder and measured the escaping Ps velocities by time of flight. We find a significant fraction of the Ps has cooled to 4 K when we use a liquid-He temperature target and positron implantation energies of 20 keV; however, more complete thermalization would require considerably higher implantation energies and possibly a transmission geometry to ensure longer contact with the cold powder.

Our present experiment is rather preliminary, but still sufficient to answer some basic questions about thermalization. The following sections will describe the apparatus, present the data, interpret the data in terms of energy spectra, and discuss the results.

II. EXPERIMENT

Our apparatus consisted of a pulsed source of slow positrons, a cooled SiO_2 powder target, a time-of-flight detector for measuring Ps velocities, and the associated electronics. Positrons were obtained from a bremsstrahlung-pair-production target[9,10] at the beam dump of an 18-MeV microtron electron accelerator.[11] The positrons were moderated to eV energies by a W(110) crystal[12] and formed into 50-nsec bunches by a pulsed 2-keV quadratic potential accelerator.[13,14] The mean kinetic energy of the 5×10^4 positrons in each bunch was about 1 keV, and the repetition rate of the bunches was 30 Hz. The positron beam was 8 mm in diameter.

The positron target was a compressed layer of fumed silica[15] consisting of roughly spherical SiO_2 grains 35 Å in radius. The layer was formed on the end of a liquid-helium transfer cold finger by coating its 25-mm-diam Cu flat end with a thin tacky layer of silicone vacuum sealing compound and pressing it with a force of about 100 N into a mound of fumed silica. The resulting SiO_2 layer was 0.3 mm thick and had a density $\rho=180(40)$ mg cm^{-3}, compared with the bulk SiO_2 density, $\rho_0\approx2.2$ g cm^{-3}.

The cold finger was surrounded by a cold shield having a 20-mm hole in the end for the positrons to pass through. Motion of the cold finger was controlled by micrometers on a 3D manipulator. An insulating glass section separated the cold finger from the rest of the vacuum system, allowing the cold finger, helium transfer lines, and dewar to be biased at potentials up to -20 kV for the purpose of accelerating the positrons into the SiO_2 powder target. The sample was baked along with the rest of the vacuum system at about 150 °C, was exposed to air for 2.5 h when it was removed to make sure the powder was unaffected, and reevacuated for 3 d without baking prior to the start of the measurements. The pressure in the vacuum can during the measurements was 1×10^{-8} torr.

The sample configuration is illustrated in Fig. 1. Inside the 100-mm-diam vacuum can a 90% W shield having a 1-mm-wide gap defines a spatial region for measuring the Ps time of flight. Outside the vacuum can a 200-mm-diam secondary Pb shield with a 4-mm-wide gap is surrounded by a 7-mm-thick by 400-mm square plastic scintillator with a 200-mm-diam hole in the center. The scintillator was coupled to two 50-mm-diam photomultiplier tubes by adiabatic light pipes on opposite sides. The anode signals were adjusted for equal amplitude and delay and added resistively at the 50-Ω input of a 125-MHz, 10^8-samples-per-second LeCroy 9400 transient recording oscilloscope. Each measurement for a given sample position, voltage, and temperature consists of a trace averaged over more than 1000 positron pulses. The averaged traces were recorded on film, and subsequently "digitized" by hand using a ruler to measure the signal amplitude at 10-nsec intervals.

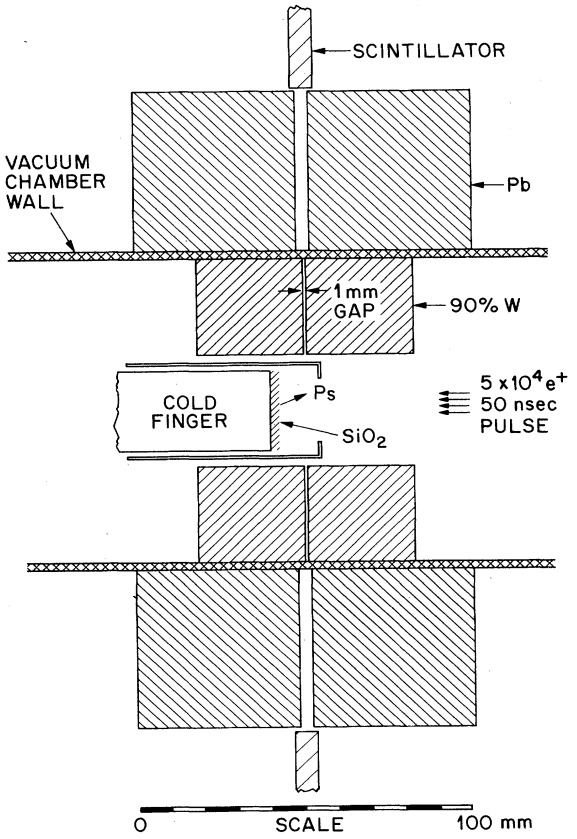

FIG. 1. Apparatus for measuring Ps velocities by time-of-flight using a pulsed positron beam.

The resolution of the slit was determined by attaching a source of 2.35-μCi ^{22}Na in pure Al at the position of the end of the cold finger, and recording the counting rate versus axial position. The maximum count rate less background was 800 sec^{-1}, and the full width at half maximum (FWHM) of the roughly Gaussian resolution curve was 1.4(1) mm, in good agreement with the 1.5 mm expected from the geometry of the 90% W slit. The maximum count rate based on the solid angle of the slit (1.0% of a sphere), the scattering in the chamber wall (14% probability of scattering) and source material (17%), and the 70% detection efficiency of 120 mm of plastic scintillator would be 823 sec^{-1} assuming that the two 511-keV gammas act as a single count due to their angular correlation. A triplet Ps atom decaying at the center of the slit would be detected via one photon from the 3γ continuum with an efficiency $\epsilon_{3\gamma}\approx2\%$.

III. TIME-OF-FLIGHT DATA

Figure 2(a) shows traces of three spectra obtained with the powder sample at room temperature[16] and located a

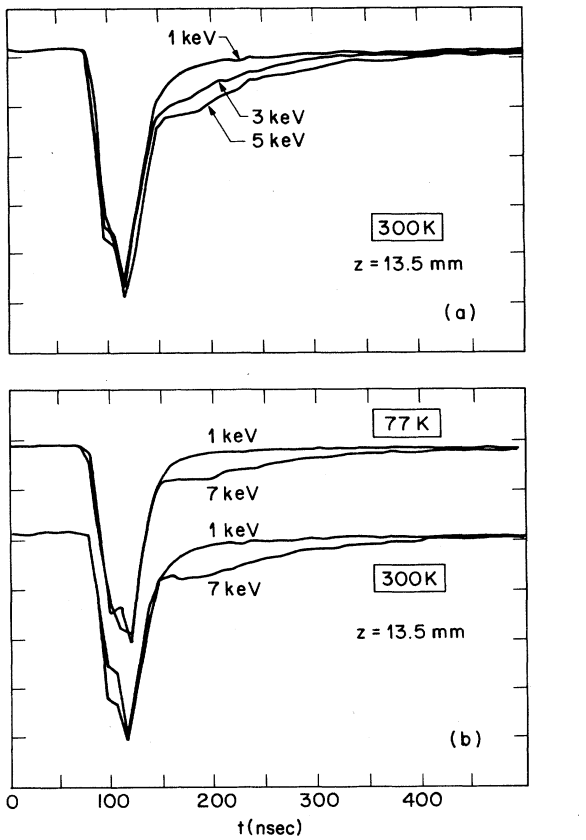

FIG. 2. Time-of-flight spectra obtained with a 9400 transient recording oscilloscope. (a) $z=13.5$ mm, SiO_2 powder at 300 K, and positrons incident at 1, 3, and 5 keV. (b) Comparison of spectra obtained at 77 and 300 K. The horizontal scale is 50 nsec per large division.

distance $z=13.5$ mm behind the midpoint of the slit. The major feature is a 45-nsec FWHM peak that we attribute to scattered γ's from the prompt annihilation of the positron pulse in the target. A delayed component that grows with increasing positron implantation energy is also visible. The wiggles in the traces are not due to counting statistics, but rather to the presence of a small-amplitude ground loop from the high-voltage pulser that we were unable to totally suppress. While the ground loop spoils the precision of the traces, they are still good enough for our present qualitative study of thermalization.

At first it seemed surprising that the amplitude of the delayed component increased as the positron energy was raised from 1 to 5 keV. However, it appears that low-energy positrons form rather energetic Ps (Refs. 6 and 17) that decays with low probability as it traverses the slit. We presume in fact that the 1-keV trace may be treated as the background signal that we may subtract from the higher-voltage traces to obtain the signal due to the partially thermalized Ps emitted from the powder surface after having undergone many collisions with the powder grains. In Fig. 2(b) we examine the effect of cooling the target and find that there is little, if any, evidence of a suppression of the shorter time component in the 77-K trace for 7-keV positrons, indicating the Ps has probably not thermalized to 300 K. Figure 3 shows two pairs of spectra for $z=2$ mm taken at 1 and 11 keV and at 1 and 21 keV. There is an obvious reduction in the amplitude of the delayed component at short times when the energy is raised, which indicates the thermalizing effect of the higher positron energy. Figure 4 shows that the delayed component at 77 K and 10 keV moves to longer times as the distance z is increased from 4 to 8 mm. The same effect as z is increased from 1 to 4 mm is visible in Fig. 5

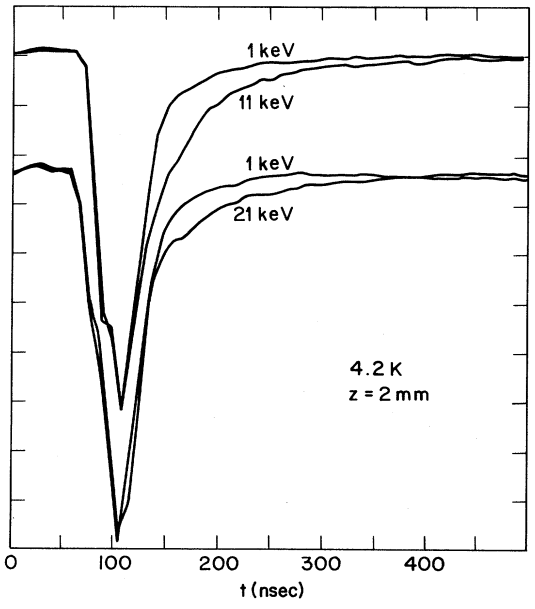

FIG. 3. Spectra obtained at 4.2 K with $z=2$ mm showing the effect of doubling the implantation energy is to reduce the amplitude of the delayed component at short times.

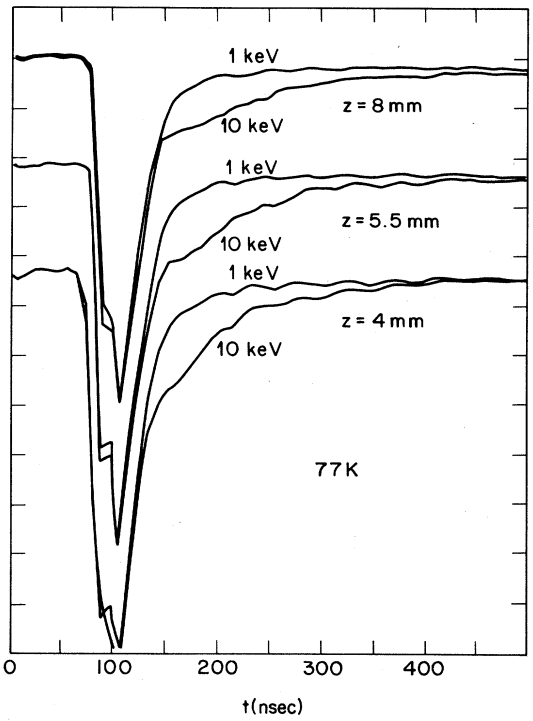

FIG. 4. Spectra obtained at 77 K and 10 keV showing that the delayed component moves to longer times as the distance z to the slit is increased.

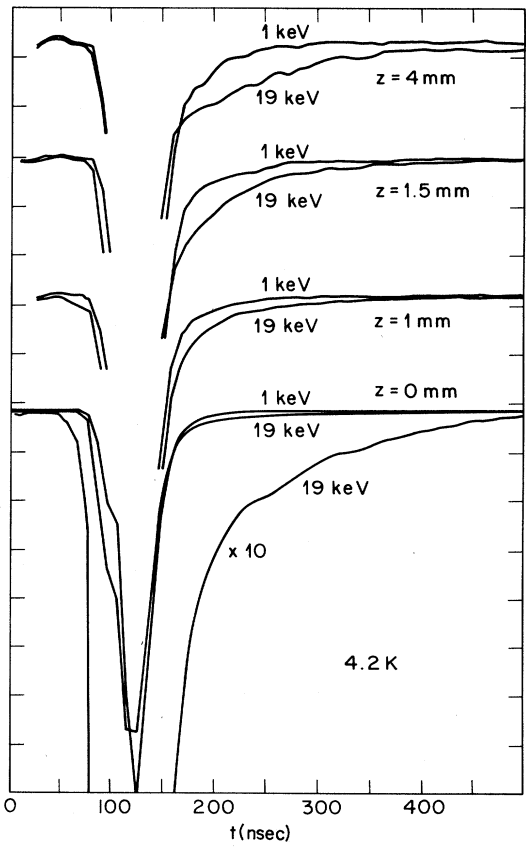

FIG. 5. Same as Fig. 4 only the sample temperature is 4.2 K and the positron energy is 19 keV.

where the sample is at 4.2 K and the positron energy is 19 keV. It is to be noted that the distances z in Figs. 2–5 were chosen so that the Ps delayed peak was reasonably separated from the prompt peak without undue attenuation due to decay in flight.

The 19-keV, 0-mm trace in Fig. 5 is also displayed with a magnification of 10 in the lowest trace. We have "digitized" this trace and displayed it in Fig. 6. The midpoint of the prompt peak defines our "$t=0$" value. The delayed component has an eyeball-fit intensity of 20% and a lifetime (dashed curve in Fig. 6) of 97 nsec if we ignore the droop at the end which might be attributable to our ground loop. Actually, the long lifetime component due to triplet Ps caught between the powder grains for unbaked SiO_2 powder in vacuum is $\gamma^{-1}\approx 140$ nsec,[3] nearly the same as the lifetime τ of triplet Ps in vacuum. The faster apparent decay in Fig. 6 is consistent with the longer lifetime and our model of Ps emission (solid line) to which we shall return later: the apparent decay rate is the sum of the annihilation rate and the rate at which Ps disappears from the detector window, which in this case corresponds to leaving the powder as well.

It is important for the interpretation of our measurements that all the traces have roughly the same vertical scale within a factor of 2. The only exception is the 0-mm one in Figs. 5 and 6 which is an order of magnitude larger because the target is being viewed directly. We infer that Ps is able to escape from the powder quite easily, even at our highest implantation energy, and that the characteristic energy[18] E_0 at which the probability of Ps escape is reduced to half of the zero energy value is at least of order 20 keV. From the median positron implantation depth[19] $x_{1/2}\approx 2\times 10^{-3}$ cm at 20 keV, we deduce that the Ps diffusion coefficient is $D\approx x_{1/2}^2/\tau\approx 30$ $cm^2\,sec^{-1}$. Since the Ps velocity is $v\approx 10^7$ $cm\,sec^{-1}$, the Ps mean-free path in the powder is $\Lambda\approx D/v\approx 300$ Å. The long mean-free path is in accord with what we estimate for Ps colliding with a gas of particles of radius $r=35$ Å, $\Lambda_{th}\approx 2\rho_0 r/3\rho\approx 200$ Å, with the exact value for Λ_{th} depending on quantum effects and how the SiO_2 particles are distributed. For example, linking the grains into branched chains[20] increases Λ_{th} to about 600 Å.

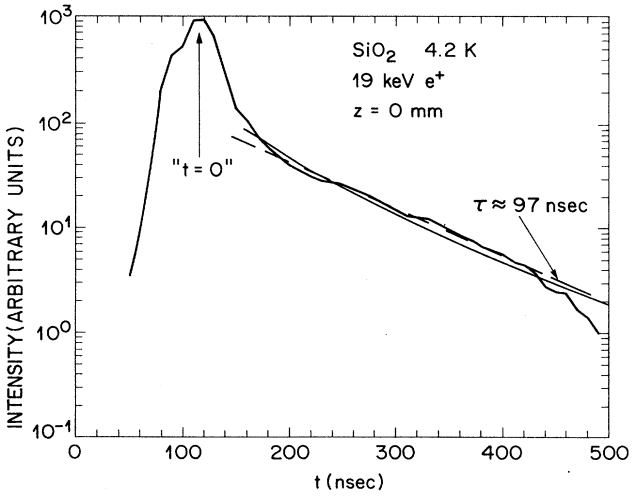

FIG. 6. "Digitized" version of the lower trace of Fig. 5, showing a delayed component attributable to Ps annihilation within the powder. The dashed line is a simple exponential. The solid line is a model curve discussed in the text.

IV. ENERGY SPECTRA

For a more quantitative examination of our data we would like to know the energy spectra of the Ps emitted by our SiO_2 target. We present in Fig. 7 the "digitized" differences between the high- and low-voltage traces in Fig. 2(b) (300-K trace) and in Figs. 4 and 5. The solid lines in Fig. 7 are from a model calculation that we discuss below. Since the Ps apparently escapes quickly from the powder, we may compute the spectra[1] of the perpendicular component of the Ps energy $E_\perp$ (ignoring the nonzero spatial and time resolution) by multiplying by $t^2e^{+t/\tau}$ and plotting the data on an energy scale. The spectra at a given temperature have been normalized to equal amplitude at one point and displayed on a log-log plot in Fig. 8. Data for times less than 40 nsec after the prompt peak were not used. At all temperatures, the spectra appear to be composed of two power-law segments: an inverse $\frac{4}{5}$ power for low energies, and perhaps an inverse-square power at high energies. For estimating the thermal and nonthermal fractions represented by Fig. 8, we combine the two inverse powers into a single normalized function with approximately the correct behavior near the crossover energy E_x. Letting $u=E_\perp/E_x$,

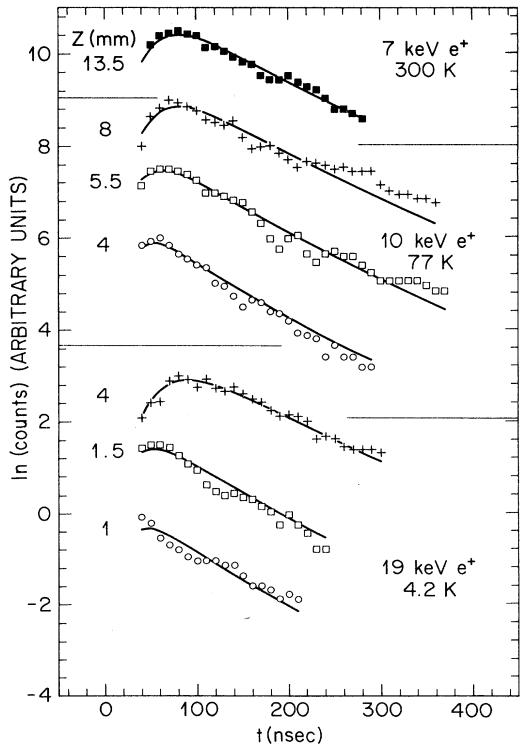

FIG. 7. "Digitized" data from Figs. 2(a), 4, and 5. The solid lines are fitted curves using Eq. (6) with parameters given in Table I.

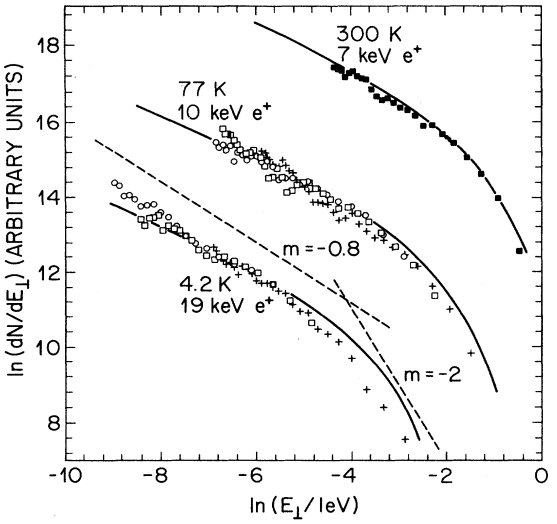

FIG. 8. Energy spectra deduced directly from the time-of-flight spectra of Fig. 7. Two power laws that appear to fit the data at high and low energies are indicated by dashed lines. The energy spectra deduced from the model fit to the data in Fig. 7 are shown by solid lines.

our approximate function is

$$\frac{dN}{dE_\perp}=5.8313\ldots(u^2+u^5)^{-2/5}. \tag{1}$$

Instead of a beam Maxwellian, or exponential spectrum with a characteristic energy given by the sample temperature, we have a power spectrum due to nonthermalized Ps. An estimate of the fraction of the positrons having a thermalized $E_\perp$ would be the integral of Eq. (1) from zero to kT:

$$f^{\perp}_{\text{thermal}}=0.857\ldots\left[\frac{kT}{E_x}\right]^{1/5}. \tag{2}$$

From Fig. 8 we estimate $E_x=192$ meV, 64 meV, and 11 meV and $f^{\perp}_{\text{thermal}}=57\%$, 54%, and 44% at 300 K, 77 K, and 4.2 K and positron implantation energies $E_+=7$ keV, 10 keV, and 19 keV, respectively. The parameters (listed in Table I) are insensitive to the exact value of E_x due to the smallness of the exponent in Eq. (2). The high-energy $1/E^2$ tails have amplitudes of about 14%. In Fig. 9 we display the lowest-energy portions of the energy spectra and dashed lines corresponding to beam Maxwellian exponentials at the temperature of the sample. The data are not inconsistent with the presence of a thermalized Ps component at each temperature.

As a further check on our interpretation, we have fitted the data of Fig. 7 using a model that includes effects due to the positron implantation profile, Ps diffusion, and the experimental time and spatial resolution. We take the implantation profile to be[12]

$$P(x)=\frac{2x}{b^2}\exp(-x^2/b^2), \tag{3}$$

with[19] $b=x_{1/2}/\ln 2\propto E_+^{3/2}$. Assuming a constant Ps diffusion coefficient D, the rate, per Ps atom initially present, of Ps emission from the surface as a function of time t will be

$$L(t)=2\Theta(t)e^{-\gamma t}Db^{-2}(1+4Db^{-2}t)^{-3/2}, \tag{4}$$

where $\Theta(t)$ is the unit step function and γ is the triplet Ps decay rate while it is diffusing among the powder grains. For definiteness we assume the spectrum of the perpendicular component of the Ps energy is a power law times a Maxwellian,

$$S(E_\perp)=E_\perp^{-m}\exp(-E_\perp/kT^*), \tag{5}$$

which gives us an expected time spectrum

$$f(t)=\text{const}\times e^{-\gamma t}\int_0^t dt'(\mu t')^{2m-2}e^{-\gamma t'}e^{t'/\tau}\times e^{-(\mu t')^{-2}}[1+4Db^{-2}(t-t')]^{-3/2}. \tag{6}$$

The slit position z and effective temperature T^* are contained in the parameter $\mu=(kT^*/m_e)^{1/2}/z$. The spatial resolution is accounted for by averaging Eq. (6) over three slit positions z and $z\pm\delta z$ with weights $\frac{1}{2}$ and $\frac{1}{4}$, respectively, and $\delta z=0.7$ mm. The time resolution was in-

TABLE I. For three conditions of positron implantation energy E_+ and sample temperature T, we list parameters E_x and $f^{\perp}_{\text{thermal}}$ fitting the directly estimated Ps energy spectrum, and parameters kT^*, m, Db^{-2}_{10}, χ^2, and $f^{\text{total}}_{\text{thermal}}$ for the model fit to the data.

Parameters	Positron energy E_+ (keV) 7	10	19
T (K)	300	77	4.2
E_x (meV)	190	64	11
$f^{\perp}_{\text{thermal}}$ (%)	57	54	44
kT^* (meV)	320±100[a]	125±38[a]	35±10[a]
m		−0.564±0.070[a]	
Db^2_{10} (nsec^{-1})		0.20±0.15 (>0.02 90% confidence)[a]	
$\chi^2_{\min}$		5.868[a]	
$f^{\text{total}}_{\text{thermal}}$ (%)	12	8	2

[a]Parameters from a simultaneous fit to all the data of Fig. 7 using Eq. (6).

cluded by a similar average using $\delta t=25$ nsec.

We have fitted the function f to the 184 observed points o_i in Fig. 7 by minimizing

$$\chi^2=4\sum_{i=1}^{184}(f_i-o_i)^2/f_i. \tag{7}$$

For the purposes of fitting, each of the seven spectra in Fig. 7 is multiplied by a constant that area-normalizes it to f over the range of the data. The free parameters in the fit were the effective temperatures T^* for each of the three conditions of sample temperature and positron energy, the exponent m, and the quantity Db_{10}^{-2} for 10 keV positrons. We fixed $\gamma=0.0074$ nsec^{-1} and found no change using values as high as 0.01 nsec^{-1}. The best-fit parameters are listed in Table I. The factor 4 in Eq. 7 was chosen empirically to make the minimum χ^2 appropriately less than the 170 expected for Poisson statistics to account for correlations and nonstatistical wiggles in the data due to the ground loop. We could only find a lower limit for the parameter Db_{10}^{-2}, corresponding to $D>20$ cm^2 sec^{-1}, in agreement with our expectation that the Ps diffusion coefficient is large.

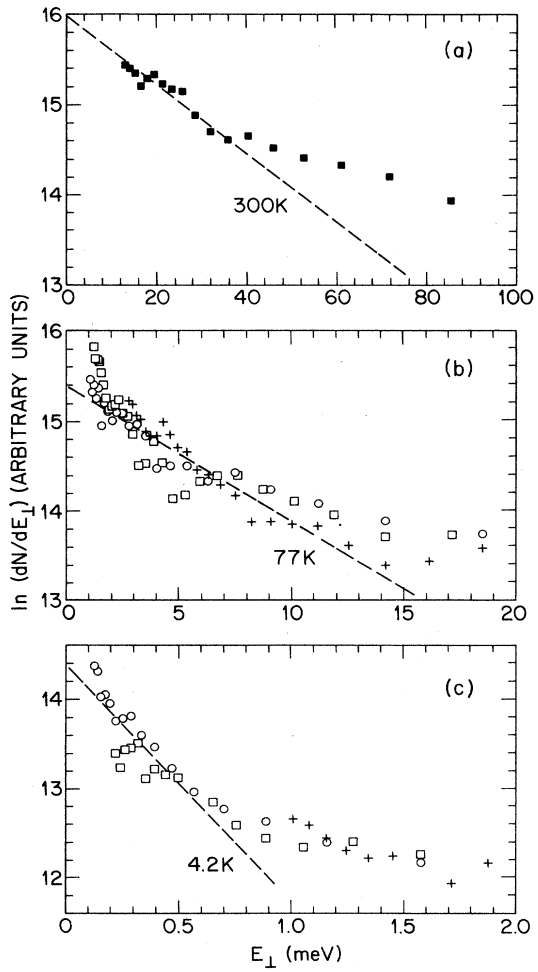

FIG. 9. Data of Fig. 8 displayed on semilog plots and showing the eyeball-fit exponential spectra (dashed lines) one would have from a beam Maxwellian at the indicated temperatures.

We may make a more meaningful estimate of the magnitude of the thermalized component by calculating the fraction of the Ps with total energy E less than k times the sample temperature. In order to proceed we must extend Eq. (5) to 3D; a reasonable choice would be

$$S(E_\perp,E_\parallel)=E_\perp^{-m}E_\parallel^{-m}\exp(-E/kT^*).$$

Integrating out the angular dependence, the spectrum of the total energy becomes

$$S(E)=E^{1-2m}\exp(-E/kT^*), \tag{8}$$

with thermal fractions

$$f_{\text{thermal}}^{\text{total}}=\left[\frac{T}{T^*}\right]^{2-2m}\Big/\Gamma(3-2m) \tag{9}$$

listed in Table I. At 4.2 K and with 19 keV positron implantation energy, the thermal fraction is only about 2%.

The solid line in Fig. 6 is an evaluation of Eq. (6) at a single slit position $z=0.5$ mm, but with the time resolution included as before. Since the curve fits the data well, we are justified in our original claim that the apparent short decay time was due to Ps time of flight and not to a disagreement with the $\gamma^{-1}=140$ nsec found by Paulin and Ambrosino. To reconcile the estimated spectrum of Eq. (1) with the more accurate Eq. (5), we have plotted in Fig. 8 the power-law Maxwellian of Eq. (5) using the best fit values of T^* from Table I. The curves have been adjusted in amplitude to make them fit the moderate-energy portion of the data. Evidently, the poor time resolution deemphasized the high-energy portion of the spectrum when we made the simple-minded energy plot directly from the time-of-flight data. The power-law part of the spectrum thus appeared steeper with $m=-0.8$, instead of the $m=-0.56$ obtained more accurately from the fit using Eq. (6). We conclude that our model explains all the data, and that Eq. (5) is a good representation of the Ps energy spectrum from the SiO_2 powder sample.

V. DISCUSSION

Unfortunately, we have no theory for how Ps loses energy to the SiO_2 powder grains. The best we can do is to construct the following picture. For large Ps energies, the average energy loss per collision is the average of the energies taken up by the various surface atoms of mass M_i upon recoiling[21] from the Ps, so that

$$dE_{\text{Ps}}=-2E_{\text{Ps}}m_{\text{Ps}}\langle M_i^{-1}\rangle dn, \tag{10}$$

where n is the number of collisions. Because the Ps is diffusing out of the sample, the average number of collisions is approximately $n=(x_{1/2}/\Lambda)^2=a^2\rho^{-2}\Lambda^{-2}E_+^3$, where[19] $a\approx4$ μg cm^{-2}. Integration of Eq. (10) is not trivial because the energy loss per collision will be reduced when the average perpendicular component of the Ps energy becomes less than the various high-frequency local modes such as the 450 meV OH stretch vibrational energy. The problem becomes simpler above a certain positron energy when the Ps energy E_{Ps} becomes comparable to the Debye energy, $k\Theta_D\approx40$ meV. At this point the average energy loss should be proportional to the

available phonon phase space, $\approx(\epsilon E_{\rm Ps}/k\Theta_D)^{3/2}$, times the atomic recoil energy, where we are assuming that the parallel component of momentum is conserved in the collision. The factor $\epsilon<1$ is to account for the necessary average over angles of incidence. We then have

$$dE_{\rm Ps}=-2E_{\rm Ps}m_{\rm Ps}M^{-1}(\epsilon E_{Ps}/k\Theta_D)^{3/2}dn. \quad (11)$$

Let us denote by E_+^D the value of E_+ for which $E_{\rm Ps}=\epsilon^{-1}k\Theta_D$. For positron energies greater than E_+^D the mean Ps emission energy becomes

$$E_{\rm Ps}(\equiv kT^*)=\epsilon^{-1}k\Theta_D\left[\frac{2}{3}\frac{E_+^3-E_+^{D3}}{E_\Lambda^3}+1\right]^{-2/3}$$
$$\approx\epsilon^{-1}k\Theta_D(\tfrac{3}{2})^{2/3}E_\Lambda^2E_+^{-2}. \quad (12)$$

Here $E_\Lambda^{-3}\equiv 2m_{\rm Ps}\langle M^{-1}\rangle a^2\rho^{-2}\Lambda^{-2}$. We plot kT^* from Table I in Fig. 10 versus E_+ and find that a power law $C\times(E_+/E_\Lambda)^{-2.2}$ fits the data over the limited range of the experiment, in rough agreement with Eq. (12). Taking $\Lambda=600$ Å and $\langle M\rangle=20m_p$ implies $E_\Lambda=8.7$ keV, allowing us to deduce that $\epsilon\approx 0.3$ from the value of the constant $C\approx\epsilon^{-1}k\Theta_D(\frac{3}{2})^{2/3}$.

Fox and Canter[22] report that in room temperature SiO_2 powder with 70-Å grain radius and density 40 mg cm^{-3} Ps begins to decay exponentially after 30 nsec. Assuming this is the time for the Ps to cool to $\approx$25 meV, we may estimate from Fig. 10 that the implantation energy corresponding to a mean Ps escape time of 30 nsec is $E_+\approx 22$ keV. The implantation energy E_0 corresponding to a mean depth equal to a diffusion length $\sqrt{D/\lambda}$ would thus be

$$E_0\approx 22\ \text{keV}(\lambda\times 30\ \text{nsec})^{-1/3}\approx 37\ \text{keV},$$

in agreement with our best fit value of $Db_{10}^2=0.2$ nsec^{-1}. We may conclude that Ps thermalization to about 5 meV in the present geometry should occur at $E_+\approx 37$ keV with a loss of half the Ps due to annihilation in the powder.

It would be interesting to do further experiments in which the positrons would be implanted into the back of a powder target so that all the Ps would have to diffuse through a thick powder layer. For large implantation energies, the linear portion of the implantation profile would tend to give an invariant energy spectrum in the front-implanted geometry of the present experiment, and would tend to inhibit thermalization. It would also be interesting to see if an efficient low-temperature Ps source could be obtained from a thick powder target directly irradiated from behind by an unmoderated positron source. It is easy to estimate that the Ps production efficiency in vacuum would be of order 1% of the source positrons.

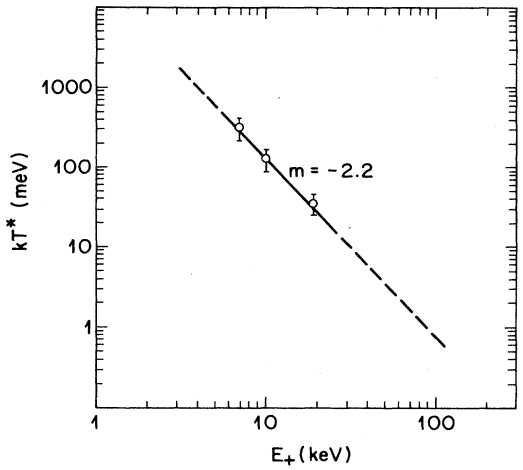

FIG. 10. Effective Ps temperature kT^* plotted vs positron implantation energy E_+. The line is an eyeball-fit power law.

The Ioffe-Regel criterion[23] for strong localization is $k\Lambda<n$, where k is the particle's wave vector, Λ is its mean-free path, and n is a constant of order unity that depends on the details of the scattering. For Ps the criterion becomes $E_{\rm Ps}<n^2\Lambda^{-2}\times 6.8$ eV, with Λ in units of the Bohr radius. With n taken to be 1, and using our estimated upper limit $\Lambda\approx 600$ Å, we would need $E_{\rm Ps}<6.8$ μeV to observe localization effects. However, the recent Platzman-Azbel[24] interpretation of the positron mobility edge in gaseous helium[25] required that $n\approx 40$. If a similar value of n applied to our SiO_2 powder target, the Ps would be localized if its kinetic energy were less than about 10 meV. We may probably exclude such a large value of n from an inspection of Fig. 8 because a significant fraction of the Ps ($\approx$30%) has thermalized below 10 meV energies in the 4.2-K, 19-keV data. A Monte Carlo calculation might allow us to reach a more definitive conclusion.

ACKNOWLEDGMENTS

The authors would like to thank Loren Pfeiffer and Phil Platzman for helpful discussions on the subjects of energy losses and localization.

[1]A. P. Mills, Jr. and L. Pfeiffer, Phys. Rev. B **32**, 53 (1985).
[2]S. Chu, A. P. Mills, Jr., and J. L. Hall, Phys. Rev. Lett. **52**, 1689 (1984).
[3]R. Paulin and G. Ambrosino, J. Phys. (Paris) **29**, 263 (1968).
[4]W. Brandt and R. Paulin, Phys. Rev. Lett. **21**, 193 (1968).
[5]S. Curry and A. L. Schawlow, Phys. Lett. **37A**, 5 (1971).
[6]D. W. Gidley, P. W. Zitzewitz, K. A. Marko, and A. Rich, Phys. Rev. Lett. **37**, 729 (1976); see also D. W. Gidley, Ph.D. dissertation, University of Michigan, 1979, available from University Microfilms, Ann Arbor, MI 48109.
[7]T. B. Chang, K. K. Deng, T. Akahane, T. Chiba, M. Kakimoto, and T. Hyodo, in *Positron Annihilation*, edited by P. C. Jain, R. M. Singru, and K. P. Gopinathan (World Scientific, Singapore, 1985), p. 974.
[8]P. Sferlazzo, S. Berko, and K. F. Canter, Phys. Rev. B **35**, 5315 (1987).

[9]D. G. Costello, D. E. Groce, D. F. Herring, and J. W. McGowan, Phys. Rev. B **4**, 1433 (1972).

[10]R. H. Howell, R. A. Alverez, and M. Stanek, Appl. Phys. Lett. **40**, 751 (1982).

[11]E. D. Shaw, R. J. Chichester, and S. C. Chen, Nucl. Instrum. Methods Phys. Res. **A250**, 44 (1986).

[12]See, for example, A. P. Mills, Jr., in *Positron Solid State Physics,* edited by W. Brandt and A. Dupasquier (North-Holland, Amsterdam, 1983), p. 432; K. G. Lynn, *ibid.,* p. 609; P. J. Schultz and K. G. Lynn, Rev. Mod. Phys. **60**, 701 (1988).

[13]A. P. Mills, Jr., Appl. Phys. **22**, 273 (1980).

[14]A. P. Mills, Jr., E. D. Shaw, R. J. Chichester, and D. M. Zuckerman, Rev. Sci. Instrum. **60**, 825 (1989).

[15]The powder was EH5 grade CAB-O-SIL made by the Cabot Corporation, Boston, MA.

[16]Note that when we state the temperature of the sample as 300, 77, or 4.2 K, we mean that the sample was at the temperature of the ambient, or that liquid N_2 or liquid He was flowing through the transfer cold finger.

[17]R. H. Howell, I. J. Rosenberg, and M. J. Fluss, Phys. Rev. B **34**, 3069 (1986).

[18]A. P. Mills, Jr., Phys. Rev. Lett. **41**, 1828 (1978).

[19]A. P. Mills, Jr. and R. J. Wilson, Phys. Rev. A **26**, 490 (1982). Note that for convenience we are assuming that the median penetration depth increases as the $\frac{3}{2}$ power of the implantation energy. The correct power may be more like 1.6 (Mills and Wilson) or 1.7 [H. E. Hansen and U. Ingerslev-Jensen (unpublished)].

[20]*CAB-O-SIL Fumed Silica,* Pamphlet C-10 (Cabot Corporation, Boston, 1968), p. 1.

[21]H. Frauenfelder, *The Mössbauer Effect* (Benjamin, New York, 1963), pp. 20–25; G. W. Ford, L. M. Sander, and T. A. Witten, Phys. Rev. Lett. **36**, 1269 (1976).

[22]R. A. Fox and K. F. Canter, J. Phys. B. **11**, 1255 (1978).

[23]A. F. Ioffe and A. R. Regel, Prog. Semicond. **4**, 237 (1960).

[24]P. M. Platzman and M. Ya. Azbel, Phys. Rev. B **36**, 2350 (1987).

[25]R. Tawel and K. F. Canter, Phys. Rev. Lett. **56**, 2322 (1986).